Palaeogeography, Palaeoclimatology, Palaeoecology 446 (2016) 19–31

Contents lists available at ScienceDirect

Palaeogeography, Palaeoclimatology, Palaeoecology

journal homepage: www.elsevier.com/locate/palaeo

Southwest Pacific sea surface conditions during Marine Isotope Stage 11 — Results from dinoflagellate cysts

Joseph G. Prebble [a,*], Erica M. Crouch [a], Giuseppe Cortese [a], Lionel Carter [b], Helen Neil [c], Helen Bostock [c]

[a] GNS Science, PO Box 30 368, Lower Hutt 5040, New Zealand
[b] Antarctic Research Centre, Victoria University of Wellington, Wellington, New Zealand
[c] National Institute of Water and Atmospheric Research (NIWA), Wellington, New Zealand

ARTICLE INFO

Article history:
Received 20 July 2015
Received in revised form 8 December 2015
Accepted 6 January 2016
Available online 13 January 2016

Keywords:
MIS11
Dinoflagellate cysts
Sea surface temperature
Productivity
Subtropical Front
SW Pacific

ABSTRACT

Dinoflagellate cyst (dinocyst) assemblages are examined from three SW Pacific marine sediment cores covering Marine Isotope Stage 11 (MIS11, 423 ka–380 ka). MD06-2988 and MD06-2989 are in the east Tasman Sea, north of the Subtropical Front (STF), whilst DSDP594 is in Subantarctic surface waters (SAW) off eastern New Zealand. Sea surface temperature (SST) estimates from dinocyst assemblages indicate that the east Tasman Sea was ~2.5 °C warmer than present during the peak warmth of MIS11. In the east Tasman Sea, north of the STF, there is a two-step warming into MIS11 in cores MD06-2988 and MD06-2989. East of New Zealand and south of the STF, at core site DSDP594, dinocyst SST estimates suggest that MIS11 was an extended warm period similar to, or slightly warmer than, present conditions, although data from the early phase (prior to 417 ka) may be compromised due to insufficient modern analogues. At all sites, glacial/interglacial climatic fluctuations were accompanied by large assemblage changes. Glacial intervals were characterised by higher abundances of assemblages typical of SAW (*Nematosphaeropsis labyrinthus*, *Selenopemphix antarctica*± *Brigantedinium* spp). Subtropical surface water (STW) assemblages dominated during the interglacial in the east Tasman Sea (including *Impagidinium aculeatum*, *I. patulum*, and *Spiniferites mirabilis*), whilst assemblages consistent with continued SAW influence remained during the interglacial at core site DSDP594, albeit with reduced cold water indicators such as *S. antarctica*. The changes are particularly pronounced in the east Tasman Sea, where the STF is inferred to have been located further north during glacials MIS12 and MIS10. The influence of STW at DSDP594 during MIS11 and the Holocene is inferred to have been less than during MIS5e. A qualitative dinocyst-based index likely reflecting primary productivity (also influenced by oxygen concentration on the sea floor) is broadly anti-phased with SST on glacial–interglacial timescales at all sites.

1. Introduction

MIS11 (423 ka–380 ka) is the first interglacial for the fully developed quasi-100 ky cycle following the climate reorganisation that took place at the Mid-Pleistocene transition, prior to which a ~40 ky cycle dominated (Clark et al., 2006; Holden et al., 2011). Unlike the subsequent shorter-duration MIS9, MIS7 and MIS5e interglacials, ice core records that span MIS11 show a sustained (~30 ka) period of Holocene-like climatic stability and mean atmospheric CO_2 close to pre-industrial levels (Siegenthaler et al., 2005). The orbital configuration was also similar to the Holocene (Herold et al., 2012; Loutre and Berger, 2003), although the Holocene contains one insolation peak so far, whilst the MIS11 interglacial extended over two insolation peaks (Rohling et al., 2010; Tzedakis, 2010).

In the New Zealand sector of the SW Pacific, published records covering MIS11 consist of sea surface temperature (SST) estimates from foraminiferal assemblage (Crundwell et al., 2008; Hayward et al., 2012; Hayward et al., 2008; King and Howard, 2000; Schaefer et al., 2005; Weaver et al., 1997; Wells and Okada, 1997; Wilson et al., 2005), estimates of dust flux into the Tasman Sea (Hesse, 1994) and a low resolution pollen record from distal marine core Ocean Drilling Programme (ODP) Site 1123 (Mildenhall, 2003; Mildenhall et al., 2004). Foraminifera-based transfer functions (Hayward et al., 2012; Hayward et al., 2008) indicate that peak MIS11 SSTs immediately west and east of New Zealand were 2–3 °C warmer than the present, and 1–2 °C warmer than the Holocene optimum. Based on this evidence, the MIS11 surface circulation pattern has been inferred to be slightly different to the Holocene, but similar to MIS5e (Hayward et al., 2012; Hayward et al., 2008).

In this study, we utilise a recently compiled Southern Hemisphere dinoflagellate cyst (dinocyst) modern dataset (Prebble et al., 2013a) to provide new insights on changes in surface water conditions during MIS11 (Fig. 1) particularly with respect to two water masses: 1) subtropical surface water (STW) of the east Tasman Sea, off the West Coast of New Zealand (cores MD06-2989 and MD06-2988),

---

* Corresponding author.
E-mail address: j.prebble@gns.cri.nz (J.G. Prebble).

http://dx.doi.org/10.1016/j.palaeo.2016.01.007

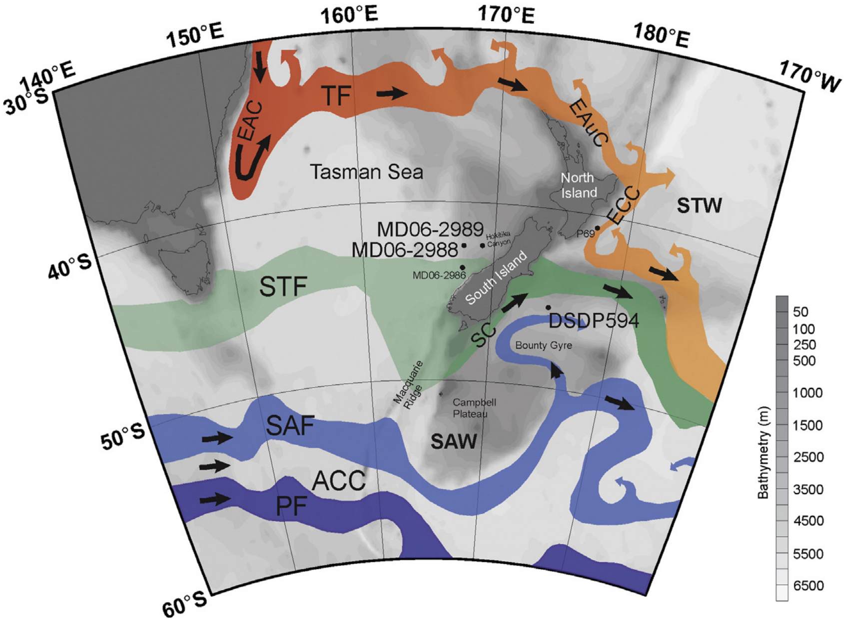

Fig. 1. Regional circulation of the SW Pacific, showing the core sites mentioned in the text. Acronyms from north to south: TF = Tasman Front, EAuC = East Auckland Current, EAC = East Australian Current, STW = subtropical water, ECC = East Cape Current, SC = Southland Current, STF = Subtropical Front, SAW = subantarctic water. SAF = Subantarctic Front, ACC = Antarctic Circumpolar Current, and PF = Polar Front. Circulation was adapted from Chiswell et al. (2015).

and 2) subantarctic surface water (SAW) east of New Zealand (core DSDP594). Due to the proximity of the cores to the Subtropical Front (STF), the data also provide insights into the position of the STF frontal system during MIS11.

2. Setting and oceanography

A major oceanographic feature of the region is the STF, which separates STW from SAW (Fig. 1). Whilst the STF is well defined east of New Zealand, it is a diffuse, meandering, double-fronted, feature in the Tasman Sea. There, it takes the form of a broad, 300–700 km wide zone, the Subtropical Frontal Zone (STFZ) (Hamilton, 2006; Smith et al., 2013). This zone is bounded to the north by a front characterised by STW overlying SAW, and to the south by another front with the reverse structure. Not only does this feature separate STW from SAW, but it also forms the boundary between two contrasting ocean circulation systems (Chiswell et al., 2015).

Compared to SAW, STW is warmer, saltier, relatively poorer in macronutrients, such as nitrate and phosphate, but is relatively enriched in micronutrients, such as iron (Boyd et al., 1999; Boyd et al., 2004), and has a mean annual SST > 15 °C and salinity > 34.5 (Chiswell et al., 2015). The annual STW primary productivity in the region generally reflects a classic spring bloom cycle, following the introduction of nutrients to surface waters by mixing during winter storms. Surface productivity is then reduced by early summer, due to the depletion of macronutrients (Boyd et al., 1999; Bradford-Grieve et al., 1997; Chang and Gall, 1998; Murphy et al., 2001; Chiswell, 2011). In contrast, SAW primary productivity in the region is limited by iron and dissolved silicon, and is dominated by picophytoplankton (organisms <2 μm), with a less pronounced seasonal bias (Boyd et al., 2004; Bradford-Grieve et al., 1999; Bradford-Grieve et al., 1997; Chang and Gall, 1998). The maximum open ocean primary productivity in the region is typically observed in the STF zone, where the mixing of STW and SAW complements the primary productivity-limiting nutrient compositions found in each contributing water mass (Bradford-Grieve et al., 1997; Murphy et al., 2001).

North of the STF is the counter-clockwise South Pacific Gyre, whose path is controlled by the Australian and New Zealand continents and regional wind fields (Chiswell et al., 2015; Heath, 1985; Roemmich et al., 2007). The northernmost part of this gyral flow is represented by a wide band of westward-flowing waters between the equator and about 30°S, with flows concentrated into several jets (Kessler and Gourdeau, 2007), some of which feed the southward-flowing East Australian Current (EAC) (Ridgway, 2007b; Ridgway and Dunn, 2003) (Fig. 1). Part of the EAC flows east across the Tasman Sea, where it forms the eddy-rich Tasman Front zone around 32°S (Chiswell et al., 1997; Ridgway and Dunn, 2003; Sokolov and Rintoul, 2009). The remainder of the EAC continues south and in recent years has strengthened markedly to extend 350 km, to southern Tasmania (Hill et al., 2008; Ridgway, 2007a). After crossing the northern Tasman Sea, the Tasman Front gives rise to a series of semi-permanent eddy and current systems, the latter flowing south along the eastern continental margin of the North Island, New Zealand, as the East Auckland and East Cape currents (Stanton et al., 1997; Tilburg et al., 2001). At ~42–43°S, the East Cape Current diverts eastwards along the northern flank of Chatham Rise, which steers the currents that potentially constrains the position of the STF to its crest (Chiswell, 1994; Uddstrom and Oien, 1999). Around the South Island, the STFZ in the Tasman Sea merges into a single front (STF), flows around the southernmost tip of New Zealand and forms the northward-flowing Southland Current (Chiswell, 1996; Sutton, 2003). The latter is also deflected eastwards as it reaches the southern flank of the Chatham Rise. Oceanographic snapshots (Sutton, 2003) indicate that the Southland Current transports mainly SAW. This would be consistent with the southern boundary of the STFZ being the main source of the Southland Current.

South of the STF, the circulation off southern and eastern New Zealand is dominated by the eastward flowing Antarctic Circumpolar Current (ACC) (Carter et al., 1998; Morris et al., 2001; Sokolov and Rintoul, 2009). The frontal systems that help define its northern limits of the ACC, namely the Subantarctic (SAF), are guided by gaps in Macquarie Ridge and steered by the pronounced topography of Campbell Plateau (Sokolov and Rintoul, 2009). En route, part of the SAF passes northwest though a gap in the Campbell Plateau to contribute to the clockwise Bounty Gyre, part of which flows along